Shape Measurement System for Roller Levelers

by

George Andres

Submitted in Partial Fulfillment of the Requirements

for the Degree of

Master of Science

in the

Electrical Engineering

Program

YOUNGSTOWN STATE UNIVERSITY

May, 2015

Shape Measurement System for Roller Levelers

George Andres

I herby release this thesis to the public. I understand that this thesis will be made available from the OhioLINK EID Center and the Maag Library Circulation Desk for public access. I also authorize the University or other individuals to make copies of this thesis as needed for scholarly research.

Signature:

_____

George Andres, Student Date

Approvals:

_____

Dr. Faramarz Mossayebi, Thesis Advisor Date

_____

Dr. Philip Munro, Committee Member Date

_____

Dr. Lin Sun, Committee Member Date

_____

Dr. Salvatore A. Sanders, Associate Dean of Graduate Studies Date

ABSTRACT

In recent years, demand for precision flatness in coiled steel has increased. This increase in demand has placed a higher importance on the outcome of roller leveling. Roller leveling is the primary method of correcting flatness defects caused from rolling the steel. The goal of this work is two-fold. The first goal is to improve upon existing roller leveler shape systems by changing the method of measuring shape defects to a "non-contact" solution that is still inexpensive. The second goal is to provide the fundamental concepts required to use adaptive control techniques to improve upon the flatness of the outgoing material. Relatively inexpensive laser or ultrasonic distance sensors are used to measure relative change in distance to the material. The relative change in distance to the material is then used to measure the fiber length of material under each sensor. A proof of concept flatness measurement system is developed and was installed. Data from the test system is analyzed and found the method of measuring shape to be acceptable.

ACKNOWLEDGEMENTS

I would like to thank my advisory committee and the faculty of the Department of Electrical and Computer Engineering at Youngstown State University.

I would also like to thank my wife Emily Andres and my daughter Lydia. Their unending support has made this work possible.

TABLE OF CONTENTS

LIST OF FIGURES

LIST OF TABLES

ABBREVIATIONS

PLC	Programmable logic controller
AC	Alternating current
PSI	Pounds per square inch
PI	Proportional plus integral controller
FIFO	First in first out buffer

CHAPTER I

INTRODUCTION

The aim of this thesis is to design a shape measurement system for a roller leveler and discuss how it could be used to control the leveler. Roller levelers are machines used to correct shape defects in coiled steel, commonly known as "strip" [1]. Currently leveling of steel is a skill that takes years for an operator to develop [1]. The goal is to measure the incoming steel shape defects, automatically adjust the leveler to correct for the incoming shape, measure the outgoing shape and change the gains (using adaptive control) to achieve flat steel. The company the author is employed by, Butech Bliss, designs, builds, installs, and commissions roller levelers for use in the steel industry[1]. Shown in figure 1 is a rendering of one of the Butech Bliss levelers.

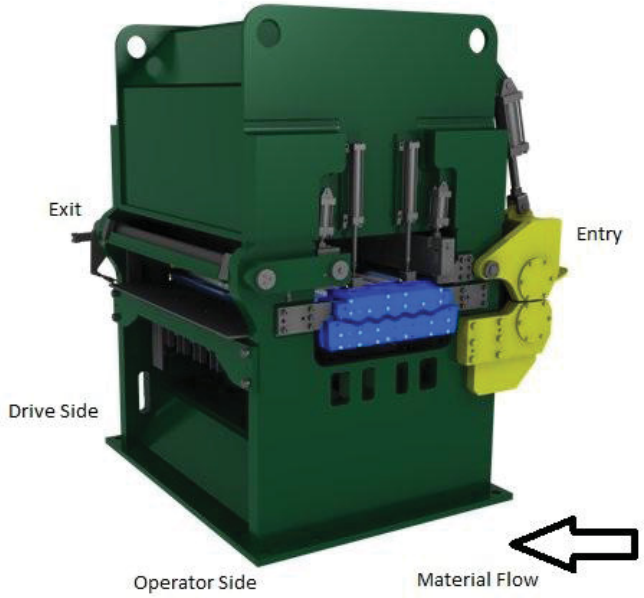

Figure 1: Rendering of a common roller leveler.

[1] The author is employed by Butech Bliss, Salem, OH 44460 USA (web: http://www.butech.com).

1.1 History

A roller leveler is the most widely adopted type of machine that is used to improve the flatness of coiled steel. Flatness variation in coiled steel has multiple causes including the steel reduction process that occurs in a rolling mill. Despite the prevalence and multiple decades of usage of roller levelers, little is known of the history of the origin of the roller leveler. More than likely, roller levelers were not any one person's or company's invention, and instead were a development that many people and companies participated in around the same time. The first U.S. patent for a roller leveler was issued in the year 1935 [2].

1.2 Motivation

The metals industry perceives roller leveling as an operating skill that is coveted [1]. Despite that skill, an operator still has a difficult time adjusting the leveler for changing shape throughout the coil. Fine tuning adjustments are required throughout the run of the coil as it winds down from a diameter of 80" to 24" at speeds up to 400 feet per minute [1, 3]. Having a roller leveler control system which can measure the shape defect and then automatically adjust to correct for changing shape, would be a great benefit for the metals industry [4]. This would significantly improve the overall consistency and quality of the strip flatness, even for skilled operators. This work focuses on developing a measurement system for the material shape that is both accurate and cost effective and then discussing how these measurements could be used to close the loop on the leveler control system.

1.3 Thesis organization

This work is divided into five chapters. Chapter II provides an overview of roller levelers and how they are used to correct shape problems in steel coils. The third chapter introduces the proposed design of this research, a roller leveler shape measurement system that could be used to control the leveler for shape correction. Chapter IV describes the hardware and software used for the proof-of-concept implementation. The final chapter presents a summary of this work as well as possible future works and applications. Several appendices provide additional tables and selected source code for the shape software.

CHAPTER II

OVERVIEW OF ROLLER LEVELING

2.1 Sources of shape problems

Roller levelers are used to correct shape defects in steel strip. There are several sources that cause shape defects in coiled steel. The most significant source of shape problems in coiled steel is the rolling mill [1, 2, 5, 3, 6]. Another source of shape problems in coiled steel is induced by the material being coiled up on itself [1, 5]. In addition, for hot rolled steel, uneven cooling of the coiled steel results in a variety of flatness issues when the coil is unwound. Typical steel coils have outside diameters that range from 36 inches to 72 inches, widths ranging from 24 inches to 96 inches, thicknesses that range from 0.040 inches to 0.75 inches, and weights ranging from 5,000 pounds to 100,000 pounds.

The primary purpose of the rolling mill is to reduce the thickness of incoming steel to a final thickness [3]. To accomplish this, the mill must apply tremendous forces to the steel. When rolling under such high forces, deflection of the work roll causes the force not to be applied evenly across the width of the steel strip [1, 2]. The perfect coil would be created when the pressure exerted upon the strip is the same across the work roll's entire width. This would lead to no strip length differentials across the width of the strip as it leaves the rolling mill. This is unfortunately a near impossibility, even with advances in mill control [5, 3].

The mill's gap is held in position by cylinders located near the ends of the work roll face. When hydraulic force is applied to the ends of the roll while material is in the mill, the work roll deflects as shown in figure 2 [5]. This leads to more strip thickness reduction near the edges of the strip, which in turn results in elongation on the edges of the strip. The extra elongation on the edges of the strip leads to a condition called edgewave as depicted in figure 3 [1].

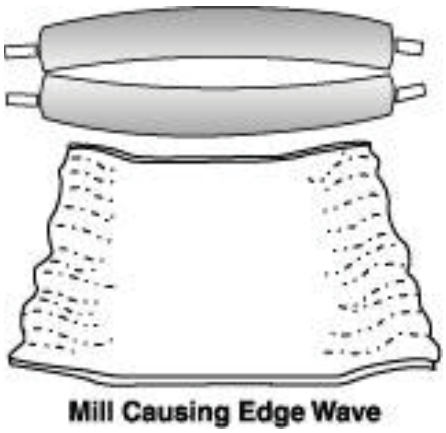

Figure 2: Mill causing edgewave.

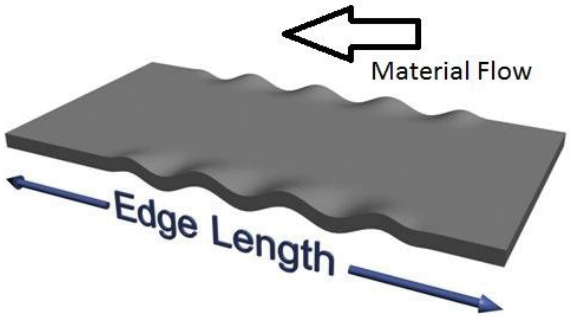

Figure 3: Edgewave.

To counteract this problem, mill work rolls typically have a crowned roll face [5]. That is, the roll face is actually thicker in the middle than on the end. However, if too much crown is in the work roll, the strip can be elongated more in the center than on the edges. This leads to a condition called centerbuckle, or "oil-canning" as shown in figures 4 and 5 [1, 5].

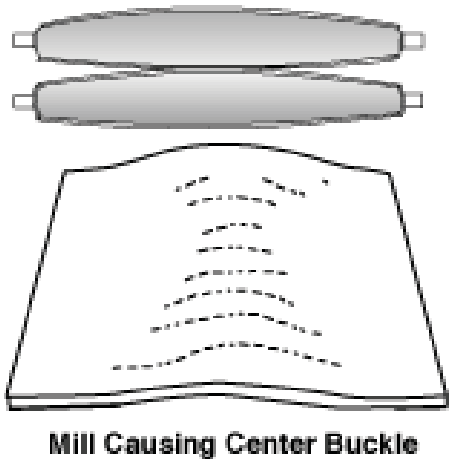

Figure 4: Mill causing centerbuckle.

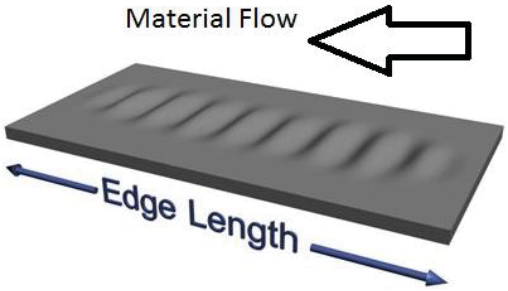

Figure 5: Centerbuckle.

When being rolled, it is important for the steel strip to be centered on the mill roll face. This is accomplished by steering the strip, as necessary to keep it on center. Steering the strip side to side while rolling is accomplished by closing the gap on one of the rolling cylinders. Closing one of the cylinders steers the strip towards the other cylinder. Consequently, more elongation would occur on the side that is closed more. This would lead to edgewave localized to either side of the strip.

Shape problems such as centerbuckle and edgewave are caused by uneven elongation across the width of the strip. If one were to cut the strip length-wise, across the width of the strip, the lengths would actually be different. The perfect strip would have all fiber lengths

equal as shown in figure 6. Strip with edgewave would have fiber lengths longer on the edges of the strip than the center of the strip as shown in figure 7. Strip with centerbuckle would have fiber lengths longer in the center of the strip than the edges of the strip as shown in figure 8. Since one cannot shrink the lengths where the shape problem is located, we must elongate the parts of the strip that are actually flat [2, 3]. This is one of the reasons that operators have a hard time comprehending the leveling process [1]. It is counterintuitive to work the part of the strip that looks flat.

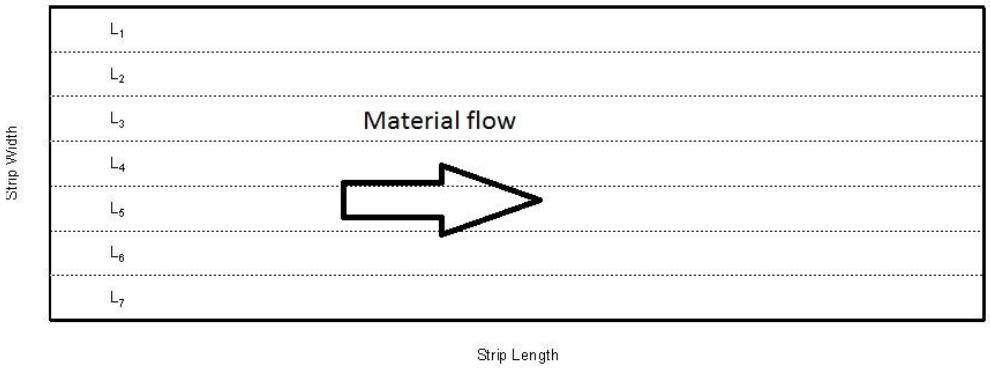

Figure 6: Perfect strip. No length differences between fibers.

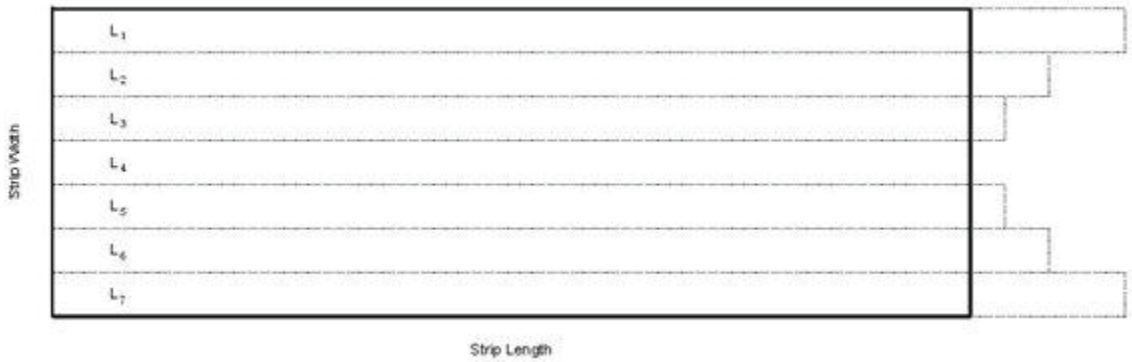

Figure 7: Edgewave. Fibers are longer on the edges than in the center.

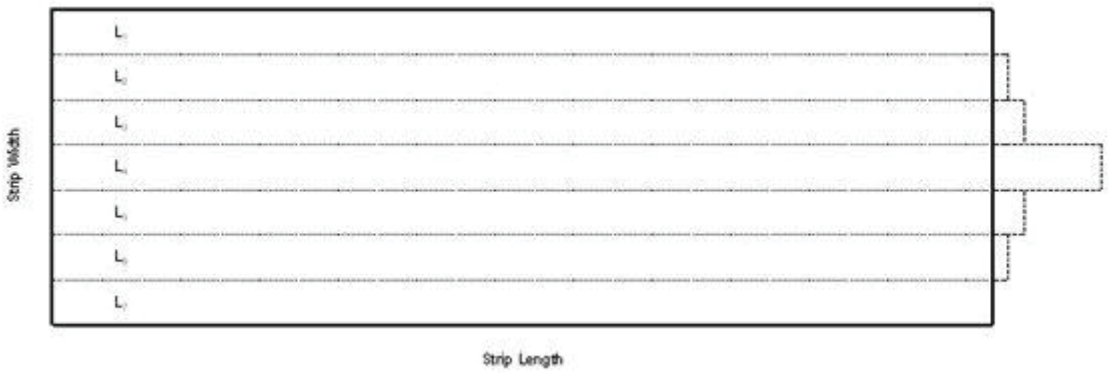

Figure 8: Centerbuckle. Fibers are longer in the center than on the edges.

Not all shape issues are due to differences in fiber lengths across the width of the strip. Coil-set, for instance, is caused by the steel being coiled to a diameter that results in a bend radius that is tighter than the elastic bend radius of the strip [1]. Under these conditions the strip is stressed beyond its yield strength, and the coiling radius remains as a permanent curvature in the strip. This shape defect is also known as "curvature" of the coil. The top surface of the strip is longer than the bottom surface of the strip due to the constant tension on the top and compression on the bottom of the strip. The coil-set of the coil becomes more severe as the coil diameter decreases while running a coil. As the diameter of the coil decreases, the more coil-set is apparent [1].

Another shape issue, crossbow, is due to differences in fiber lengths across the width of the strip. Crossbow occurs when the fiber widths on the top surface of the strip are longer than the fiber widths on the bottom surface of the strip. Since roller levelers chiefly correct for shape defects across the length of the strip it has to work the entire width of the strip to correct for crossbow.

2.2 Description of roller levelers

Roller leveler work rolls can be positioned by jacks or wedges or hydraulic cylinders. A typical hydraulic cylinder controlled roller leveler consists of the following:

1) Fixed upper backup rolls, as shown in figure 9, item a [7].
2) Individually adjustable lower backup rolls, often referred to as flights, as shown in figure 9, item c [7].
3) Hydraulic cylinders, one entry and one exit, per flight, used to control the lower backup rolls, as shown in figure 10 [1].
4) Changeable work roll cassettes that have different size driven work rolls, as shown in figure 9, item b [7].

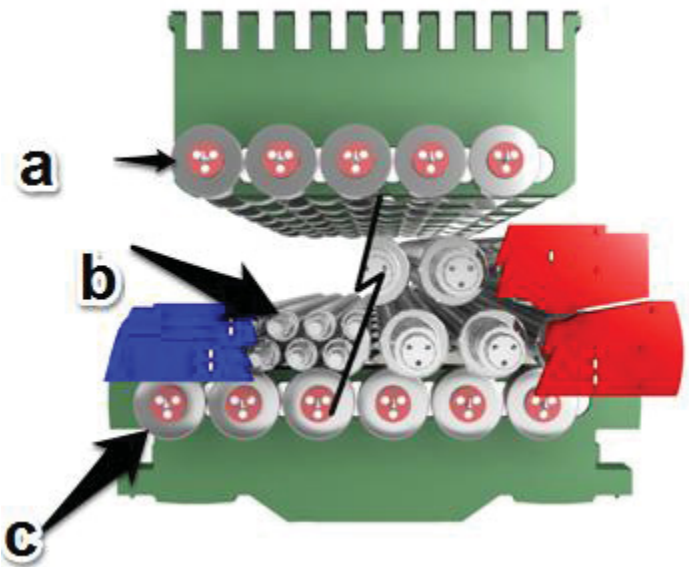

Figure 9: Roll nest of a cassette leveler. (a) Fixed upper backup rolls. (b) Interchangeable work roll cassettes. (c) Individually adjustable lower backup rolls.

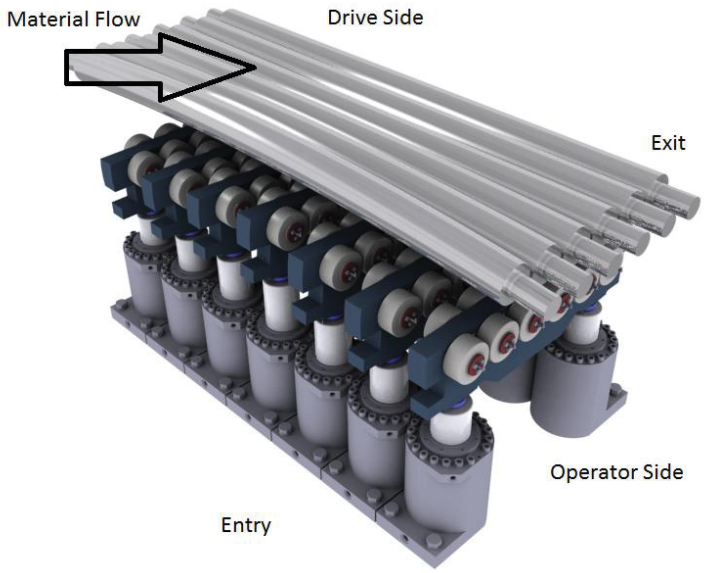

Figure 10: Entry and exit cylinders adjusting the lower backup rolls or flights.

The fixed upper backup rolls, as shown in figure 9 item a, are non-driven rolls that have a function of supporting the forces from the work rolls that reside in the cassette [1, 7]. The top half of the changeable work rolls are clamped up to the upper backup rolls to form a nest.

The moveable lower backup rolls, as shown in figure 9 item c, often referred to as flights, are controlled by hydraulic cylinders as shown in figure 10 [1, 7]. Each flight has an entry and exit cylinder attached to it. The entry and exit cylinders are each controlled separately. The lower half of the changeable work roll cassette, as shown in figure 9 item b, sits on top of the flights. When all the flight cylinders across the entry end of the leveler are moved to the same vertical position, they establish the entry roll gap between the upper and lower work rolls. Because the work rolls are uniformly supported there is no bending of the work roll face. In addition to the above, the flights can also move up and down relative to each other, and can be positioned so that they do not uniformly support the lower work roll. When the strip passes over this roll it creates forces against the work roll. Since the roll is

not uniformly supported, it will bend until it encounters a backup roll. [7, 3]. This bending only takes place when a complete roll nest is created. A complete roll nest would be created when steel is in the leveler and significant force is applied to it through the nest.

The changeable work roll cassette, shown in figure 9 item b, consists of the aforementioned top and bottom groups of work rolls. These top and bottom groups of the work rolls can be removed together as one cassette. This allows different work roll sizes to be used for different thicknesses and strengths of material. In the example leveler, each one of the work rolls is individually driven by an AC motor and drive. Individually driven work rolls allow for speed differences among the rolls, which must occur due to the nature of the deeper plunge on the entry work rolls versus the plunge on the exit work rolls.

2.3 Operation of roller levelers

As the strip passes through the leveler it reverse bends, up and down as it passes between the upper work rolls and the lower work rolls. The degree of bending is more severe at the entry of the leveler and gradually tapers to virtually no bending of the strip as it exits the leveler. The degree of bending is established by the amount of plunge of the entry work rolls. During bending, the strip is subjected to alternating forces of compression and tension as shown in figure 11 [2, 8, 6, 9]. If the bend radius is pointing upwards, the top surface of the strip is subject to tensile stresses and strains. The subsequent bend is in the reverse direction and the top surface is subject to compressive stresses and strains. At any given bend the bottom surface is subjected to stresses and strains that are in the opposite direction of the top surface of the strip. The neutral axis does not see any change in stress or strain. The

neutral axis is generally in the middle of the thickness of the strip. By definition, tensile forces are forces that are acting to stretch the material, and compression forces are forces that are acting to push the material together. The tensile forces occur on the material farthest away from the work roll that is being acted upon. The compression forces occur on the material nearest the work roll that is being acted upon. The more the work rolls are plunged, the more bending force is applied to the strip.

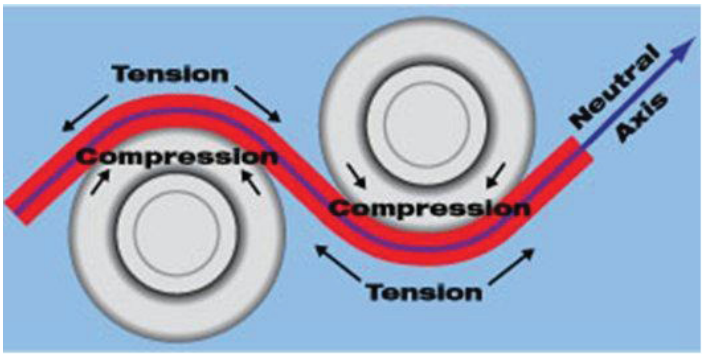

Figure 11: Cross-sectional area of steel in compression and tension.

The distance between the bottom of the top work rolls and the top of the bottom work rolls is called the "gap" [1]. In general, the entry gap is set tight and the exit gap is set at the thickness of the material being leveled [7, 3, 6].

For a roller leveler to accomplish its job, the strip must be bent beyond the yield strength of the strip [2]. The yield point is the stress (often measured in psi, or pounds per square inch) at which the material is plastically deformed [8]. Bending resulting in stresses less than the material's yield point accomplishes no plastic deformation. In this case, the work done is elastic and the material will spring back to its initial shape. The yield point is clearly marked on the stress versus strain curve as depicted in figure 12 [8]. The material is said to be yielded one strain when it is subjected to a stress at the yield point. Associated with the yield stress is the yield strain, which is the change in length of the strip at the yield

point. In the elastic region, the stress and the strain are linearly associated with each other. This relationship is called the modulus of elasticity. The modulus of elasticity is the slope of the straight line in the elastic region of the stress strain curve as depicted in figure 12 [9]. For instance, the modulus of elasticity at room temperature (70 degrees Fahrenheit) is 30 million pounds per square inch for carbon steel.

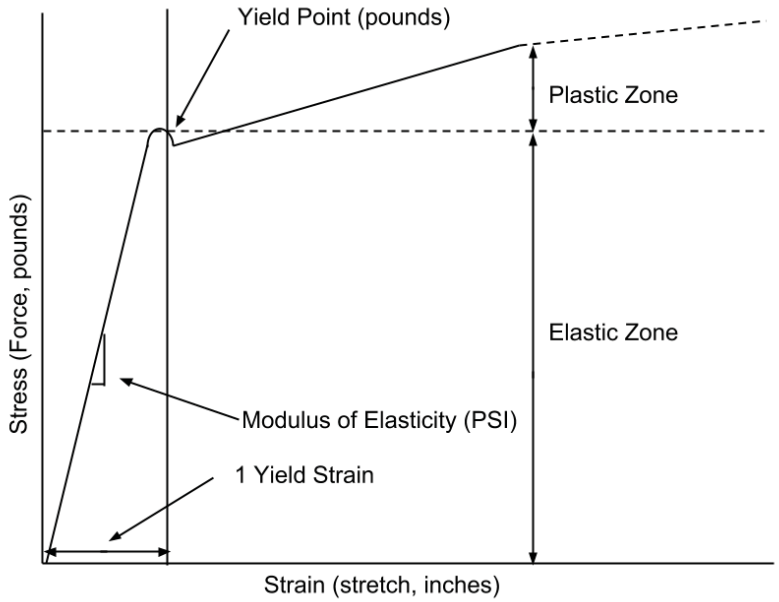

Figure 12: A typical stress versus strain curve for steel.

The number of yield strains is a value referring to the total strain the strip has been subjected to; divide by the value of one yield strain. For example, for a steel strip with yield strength of 50,000 psi the corresponding yield strain is 50,000 psi /30,000,000 psi, which is .001667 in/in. If while roller leveling, the strip is subjected to a strain of .00833 inches, then it would have seen 5 yield strains. When looking at the cross-sectional area of the steel, the fibers furthest from the center of the thickness of the strip are subjected the highest strains and therefore the easiest to correct. The fibers closest to the center of the thickness of the

strip, are much harder to correct. The amount of the cross sectional area of the material that is yielded is called percent material yielded.

The percent material yielded is related to the number of strains that the material is subjected to. This relationship is described in (1) where: 1) *Y* is the percent cross sectional material yielded; and 2) *NS* is the number of yield strains work done on the material. Equation (2) describes an example where five yield strains of work is done on the material to yield 80 percent of the cross sectional area.

$$Y = \left(\frac{NS - 1}{NS}\right) \times 100 \tag{1}$$

$$Y = 80\% = \left(\frac{5 - 1}{5}\right) \times 100 \tag{2}$$

Based on prior experience, Operators of roller levelers have developed "rules of thumb" for correcting flatness defects in strip. The rule of thumb for correcting coilset is to yield 50 percent of the cross sectional area of the material, or to work the material two yield strains as shown in (3) [8]. Since coil-set is not caused by a fiber length difference across the width of material, the method for correcting it is to plunge equally across the width [1].

$$Y = 50\% = \left(\frac{2 - 1}{2}\right) \times 100 \tag{3}$$

The general rule of thumb to try and correct crossbow using a roller leveler would be to yield 80 percent of the cross sectional area of the material, or to work the material five yield strains as shown in (4) [8]. Since crossbow is caused by a top to bottom surface fiber length difference across the width of material, the method for correcting it requires deeper plunges. When compressing material in one direction, the material expands in the directions perpendicular to the direction of compression. The ratio of the amount of expansion distance compared to the amount of compression distance is referred to as Poisson's ratio. Poisson's

ratio for typical grades of steel is 0.3. This implies that if we are loading an element in the longitudinal direction, the effectiveness in the width direction is reduced by a factor of 0.3. Since the leveler work roll plunge is in the longitudinal direction, deeper plunges are required for correcting crossbow.

$$Y = 80\% = \left(\frac{5-1}{5}\right) \times 100 \tag{4}$$

Calculating what the work roll gap should be to level a certain material depends on the diameter and spacing of the work rolls. One method of calculating the work roll gap is described in (5) and (6) [3].

$$G_E = \left(\frac{YS \times (CD)^2}{12 \times (1-Y) \times \left(\frac{t}{2}\right) \times E}\right) - t \tag{5}$$

$$G_X = t \tag{6}$$

where

E	modulus of elasticity for material (psi);
t	thickness of material (inches);
Y	percent of material yielded;
YS	yield strength of material (psi);
G_E	gap between the entry work rolls to yield the percentage indicated (inches);
G_X	gap between the exit work rolls (inches);
CD	center distance between rolls (inches).

As stated before, centerbuckle is a shape that occurs when the center fibers of the material are longer than the fibers near the edges. This causes the material in the center to buckle as the material moves. To correct for this shape defect the fibers near the strip edges have to be stretched to match the length of the fibers in the center of the material [2]. As depicted in figure 13, lengths A and B should be the same length to correct for centerbuckle. To accomplish this, the flights near the edges of the material need to be plunged deeper than

the flights in the center of the material [7]. This will bend the bottom half of the work rolls into a smile shape that will stretch the outside fibers.

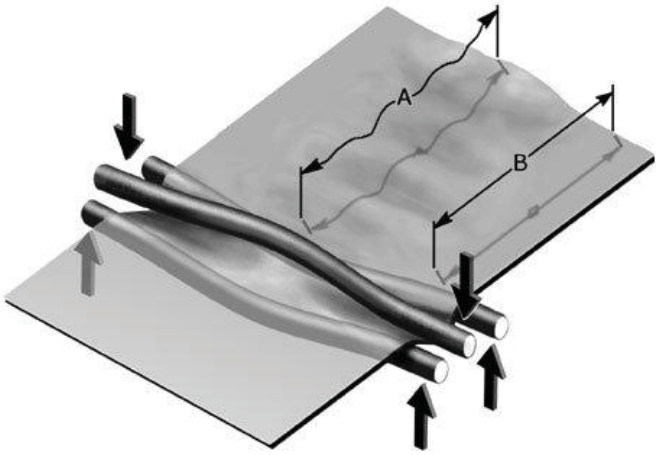

Figure 13: Rolls adjusted to correct for centerbuckle.

Edgewave is a shape that occurs when the fibers near one or more edges of the material are longer than the fibers near the center of the material as shown in figure 14. To correct for edgewave on both sides of the strip, the fibers near the center of the material need to be stretched to match the length of fibers at the edges of the material [2]. To accomplish this, the flights near the center need to be plunged deeper than the flights on the edges [7]. This will bend the bottom half of the work rolls into a frown shape. To correct for edgewave on one side of the strip, the fibers near the center and the opposite edge need to be stretched to match the length of fibers at the edge of the material. To accomplish this, the flights near the center and the opposite edge need to be plunged deeper than the flights on the edge with the shape defect. This will bend the bottom half of the work rolls into a lopsided frown shape.

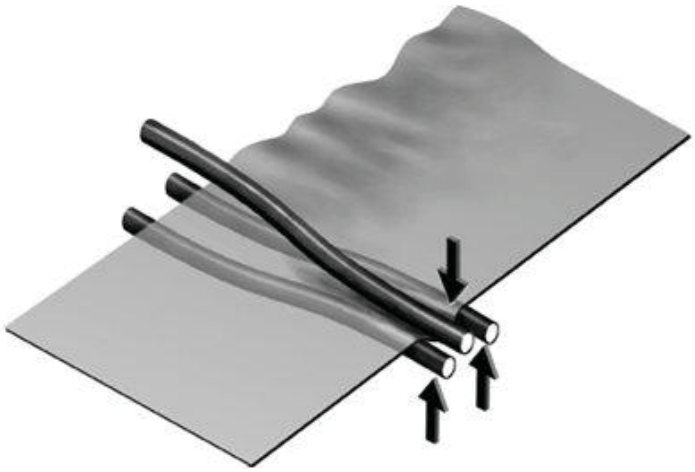

Figure 14: Work rolls adjusted for correcting edgewave localized to one side of steel.

2.4 Offset versus plunge

The rule of thumb for correcting certain shape defects was previously stated. The shape defect coilset requires the leveler to be plunged at least 2 yield strains to be corrected. The shape defect crossbow requires the leveler to be plunged at least 5 yield strains of plunge to be corrected. The general method of how to offset the individual flights has also been mentioned to correct for edgewave and centerbuckle. However, if the individual flights were offset to correct for edgewave or centerbuckle without having the leveler plunged deep enough, the ability to correct shape would be dampened. For sake of brevity, in this work we are only considering measurement of length differences and assuming that the plunge is set correctly to correct for coilset and crossbow.

CHAPTER III

PROPOSED MEASUREMENT AND CONTROL TECHNIQUE

3.1 Overview

In order to adequately remove the shape defects, first the incoming shape must be measured [3]. Once the incoming shape is known then the leveler will have to be set to correct it. After correction the shape should again be measured as a feedback to the shape control system. If the shape cannot be measured after the leveler, then the operator's adjustment of the flights should be used as feedback to the shape control system. This control should change throughout a coil depending on incoming shape and feedback shape.

3.2 Techniques for shape defect measurement

Shape defects in strip are caused by uneven elongation across the width of strip. Measuring the shape of the strip is achieved by measuring the relative lengths of the fibers across the width of strip or by measuring the stresses in those fibers. One approach to accomplish this would be to install a shape roll that measures the pressures across the width of a segmented roll [3]. The downside of this measurement technique is that the sensors

could be damaged if the force on them is too great [3]. Also, the measurement of shape can be incorrect if the force on them is not great enough [3].

Another method of measurement is to use a contact position displacement sensor [3]. This, however, has the downside of requiring the material to be sufficiently wrapped around the roll. To be sufficiently wrapped, the material has to be under tension [3]. This is not always an easy task when it comes to material thicknesses greater than 0.5 inches. A contact sensor would also have to deal with vibration issues, which could affect the measurement [4]. An ideal way to measure the strip would be a non-contact solution.

A series of non-contact distance sensors could be used to measure distance to the strip at multiple points across the strip's width, as shown in figure 15. One could then buffer the distances of the sensors in the controller and analyze them at some interval to obtain the amplitude and period of the sine wave created by the sensor data. However, this takes time and lots of processing power that most controllers (programmable logic controllers) used in manufacturing plants, do not have. To solve the problem of the lack of processing power, there is a very simple equation that can be used to calculate the lengths of material in the fibers entering a leveler.

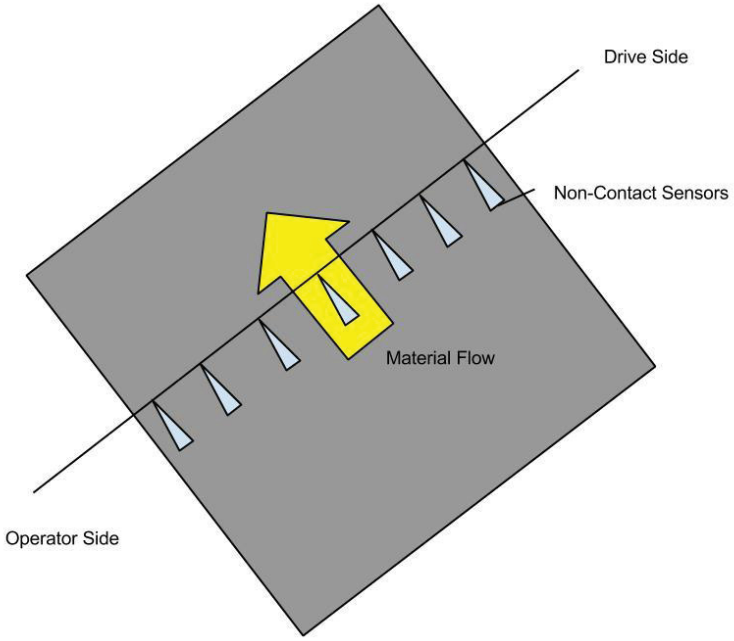

Figure 15: Non-contact sensors mounted across the width of material.

The length of material entering the leveler can be calculated using a non-contact distance sensor and a simple equation. The actual distance of the strip from the sensor does not matter. All that matters is the relative change in distance between scans of the controller. Using this change in sensor value between scans, as shown in figure 16, we can use the equation for distance between two points with small modifications to calculate the amount of material that has passed under the sensor as shown in (7).

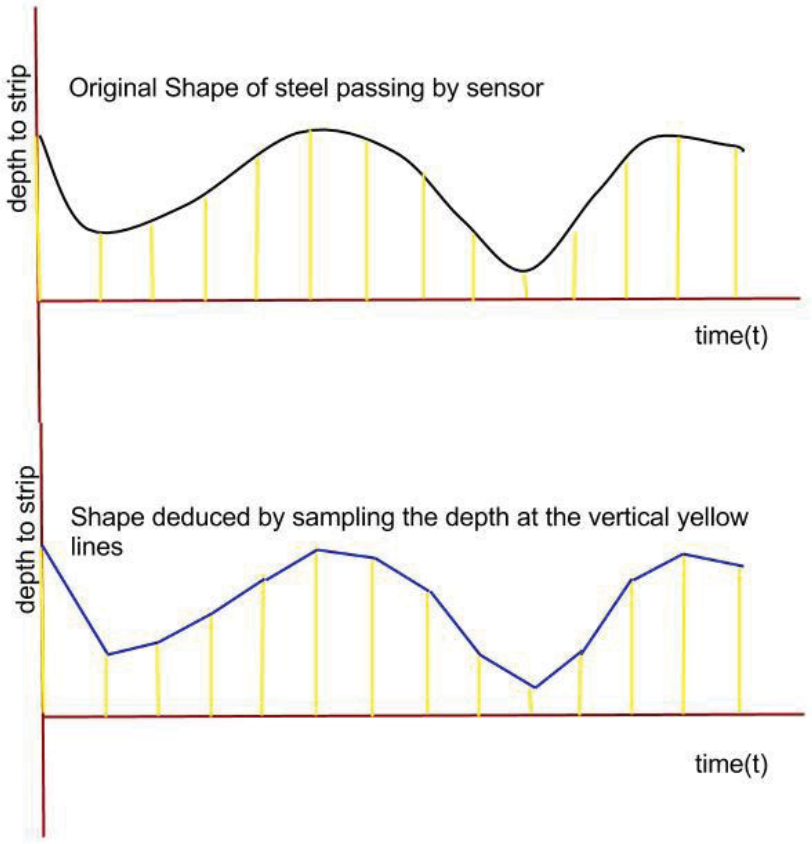

Figure 16: Actual depth to steel versus calculated depth measured by flatness system.

$$L = \sum_{i=1}^{n} \sqrt{(h_i - h_{i-1})^2 + v_i{}^2 \cdot (t_i - t_{i-1})^2} \tag{7}$$

where

h_i distance from the sensor to the strip at sample *i* (inches);
v_i velocity of the strip at sample *i* (inches / second);
t_i time at sample *i* (seconds);
L length of the strip passing beneath the shape system after *n* samples (inches).

If we have some non-contact distance sensors mounted across the width of the strip, as shown in figure 15, we can measure the lengths of material passing beneath using (7). We can then compare the differences in lengths of the fibers at some length interval. This length

interval is known as the evaluation length. These differences in lengths can help us identify the shape defects present as the material enters the leveler.

As stated before, if the lengths of the fibers on the edges of the strip are longer then edgewave is present on both sides as shown in table 1 and figure 17. Tables 1, 2 and 3 contain length differential data for different shape defects. The x column of the tables represents distance from centerline of the non-contact sensor, in inches. The y column of the tables represent length difference of material passing underneath each sensor over a given evaluation length, in inches. If the lengths of the fibers in the middle of the strip are longer then centerbuckle is present as indicated in table 2 and figure 18. If one edge has longer fibers than the center or the opposite edge then edgewave is present only on one edge as shown in table 3 and figure 19.

Table 1: Length differential data for edgewave on both sides of the steel.

x (inches)	y (inches)
-30	-0.2
-20	-1.0
-10	-2.2
0	-3.2
10	-2.4
20	-0.7
30	0.0

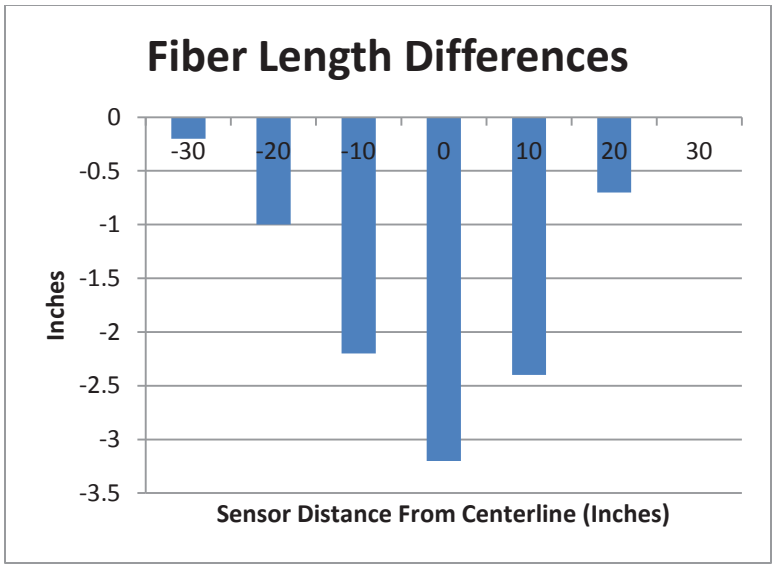

Figure 17: Length differential chart for edgewave on both sides of the steel.

Table 2: Length differential data for centerbuckle.

x (inches)	y (inches)
-30	-2.8
-20	-2.1
-10	-0.8
0	0.0
10	-0.9
20	-1.8
30	-3.0

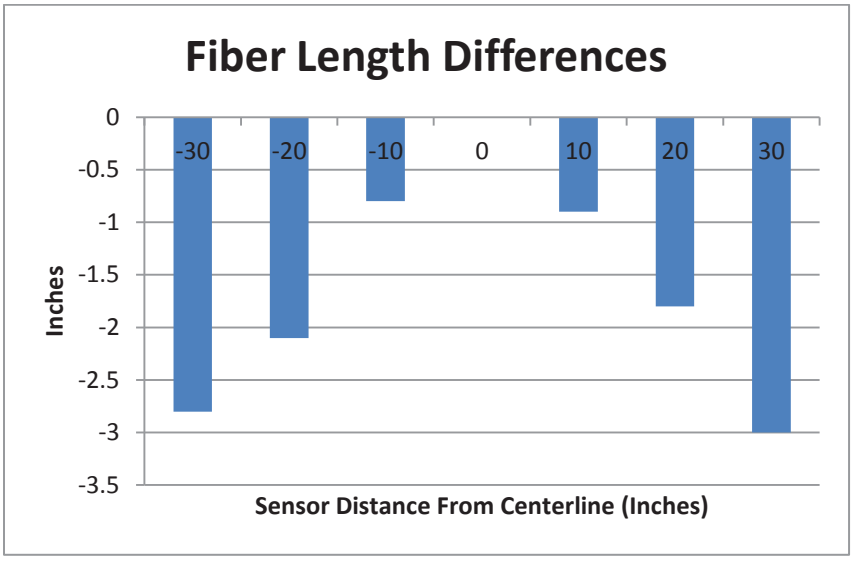

Figure 18: Length differential chart for centerbuckle.

Table 3: Length differential data for edgewave localized to one side of the steel.

x (inches)	y (inches)
-30	-2.5
-20	-2.7
-10	-2.9
0	-3.0
10	-2.5
20	-1.2
30	0.0

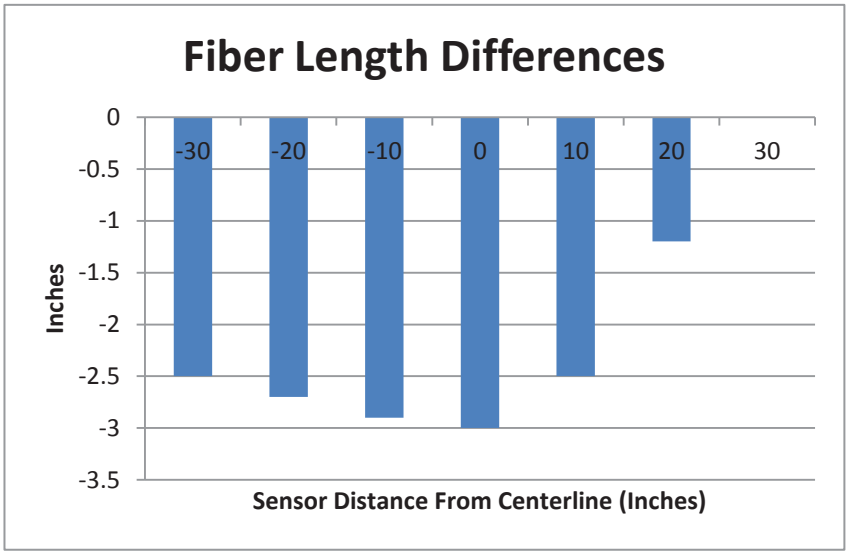

Figure 19: Length differential chart for edgewave localized to one side of the steel.

The evaluation length of material at which the shape is calculated, should be chosen to be enough data points to effectively filter out any noise in the system. However, if we only evaluate the flatness at this evaluation length, then we may have the commanded offsets change quite significantly at the time of evaluation. To alleviate this, the sensor data should be stored in a FIFO (first in first out) buffer at a much smaller length than the evaluation length. This length is called the sample length. For instance if the evaluation length were 48 inches and the sample length is 1 inch, the system would fill the FIFO buffer with 48 entries

of data and then evaluate the shape every 1 inch after that. The last 48 entries in the FIFO buffer are always used for the shape calculation. This would filter out any noise and should give a much smaller offset change over the next 48 inches rather than making one large offset change every 48 samples.

3.3 Technique for correcting shape problems

Now that the shape problem entering the leveler is known we must set up and control the leveler to fix the shape problem. The length that needs to be elongated at each flight is known from section 3.2. This length is multiplied by a gain to calculate the commanded offset position (inches). The operator will be notified if the leveler is not setup to a minimum of 3 yield strains plunge. If the plunge is not sufficient enough, no amount of individual flight offset could fix the shape defect.

Figure 20 depicts the entry flatness sensor array control diagram. Inputs to the control are entry strip speed, the height to the strip from all of the entry flatness non-contact sensors, and the time between scans. An array of entry fiber lengths is calculated as shown in (8). Equation (9) results in the maximum entry fiber length. The array of entry fiber length error is the difference between the maximum entry fiber length and the array of entry fiber lengths, as shown in (10). Equation (11) results in the entry fiber length percentage error array. The entry fiber length percentage error array is multiplied by the entry flatness system proportional gain to calculate the entry flight calculated position offsets array as shown in (12). The entry flatness system proportional gain would be scaled such that the output would be the amount offset per flight that would correct for the incoming shape error.

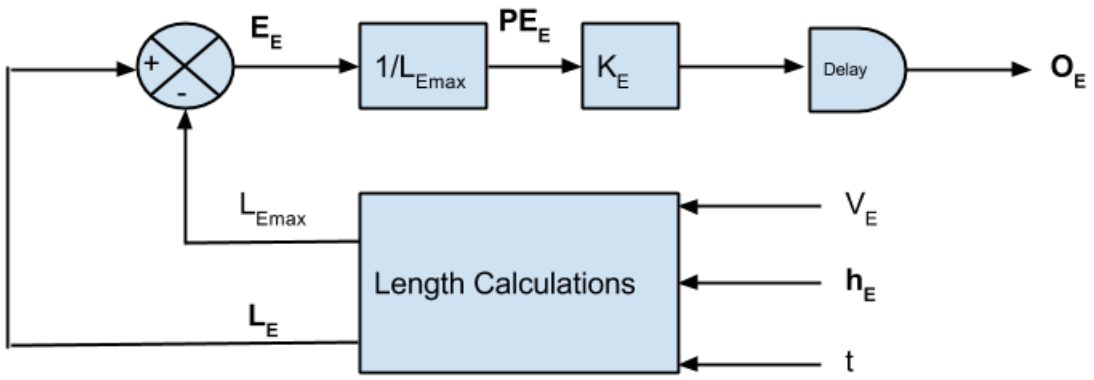

Figure 20: Control diagram for entry flatness sensor.

$$\boldsymbol{L_E} = \begin{bmatrix} \sum_{j=1}^{m} \sqrt{\left(h_{E0,j} - h_{E0,j-1}\right)^2 + {v_{Ej}}^2 \cdot \left(t_j - t_{j-1}\right)^2} \\ \sum_{j=1}^{m} \sqrt{\left(h_{E1,j} - h_{E1,j-1}\right)^2 + {v_{Ej}}^2 \cdot \left(t_j - t_{j-1}\right)^2} \\ \sum_{j=1}^{m} \sqrt{\left(h_{E2,j} - h_{E2,j-1}\right)^2 + {v_{Ej}}^2 \cdot \left(t_j - t_{j-1}\right)^2} \\ \vdots \\ \sum_{j=1}^{m} \sqrt{\left(h_{En-1,j} - h_{En-1,j-1}\right)^2 + {v_{Ej}}^2 \cdot \left(t_j - t_{j-1}\right)^2} \end{bmatrix} \tag{8}$$

where

$\boldsymbol{L_E}$	entry fiber lengths of n backup flights (inches);
$h_{En,j}$	entry sensor height, flight number n, sample number j (inches);
v_{Ej}	entry strip speed, sample number j (inches per second);
t_j	time at sample j (seconds);
n	number of flights;
m	total number of samples;
j	current sample number.

$$L_{Emax} = \max\left(L_{E0}, L_{E1}, L_{E2}, \ldots, L_{En-1}\right) \tag{9}$$

where

L_{Emax} entry maximum fiber length (inches);
L_{En} entry fiber length of flight *n* (inches);
n flight number.

$$\boldsymbol{E_E} = \begin{bmatrix} L_{E0} - L_{Emax} \\ L_{E1} - L_{Emax} \\ L_{E2} - L_{Emax} \\ \vdots \\ L_{En-1} - L_{Emax} \end{bmatrix} \tag{10}$$

where

$\boldsymbol{E_E}$ entry fiber length error (inches);
L_{En} entry fiber length of flight *n* (inches);
L_{Emax} entry maximum fiber length (inches);
n flight number.

$$\boldsymbol{PE_E} = \begin{bmatrix} E_{E0}/L_{Emax} \\ E_{E1}/L_{Emax} \\ E_{E2}/L_{Emax} \\ \vdots \\ E_{En-1}/L_{Emax} \end{bmatrix} \tag{11}$$

where

$\boldsymbol{PE_E}$ entry fiber length percentage error (%);
E_{En} entry fiber length error of flight *n* (inches);
L_{Emax} entry maximum fiber length (inches);
n flight number.

$$\boldsymbol{O_E} = \begin{bmatrix} PE_{E0} \cdot K_E \\ PE_{E1} \cdot K_E \\ PE_{E2} \cdot K_E \\ \vdots \\ PE_{En-1} \cdot K_E \end{bmatrix} \tag{12}$$

where

$\boldsymbol{O_E}$	entry flight calculated position offset (in);
PE_{En}	entry fiber length percentage error of flight n (%);
K_E	entry flatness system proportional gain;
n	flight number.

The entry flight calculated position offset array is buffered in a FIFO register every sample length. The size of the FIFO register is the number of samples of sample length needed to achieve the distance between the entry flatness sensor and entry of the leveler. For instance, if the length between the entry flatness sensor and the entry of the leveler is 30 inches and the sample length is 1 inch, then the size of the FIFO register would be 30 samples. The commanded entry offsets are unloaded from the FIFO every sample length once the FIFO has become full.

3.4 Adaptive control feedback from exit sensors

The leveler is now setup to attempt to correct for the incoming shape defect. However, how do we know that the gain we have set for our control is adequate? Does the gain need to change for different materials? There are two options that could be considered for this. One option is to put another bank of shape sensors after the leveler, and the second is to use the operator's manual adjustments as the feedback we need.

By using a duplicate bank of sensors at the exit of the leveler, the effectiveness of the entry flatness system could be evaluated as shown in figure 21. Inputs to the control are exit

strip speed, the height to the strip from all of the exit flatness non-contact sensors, the time between scans, and the entry flatness system proportional gain. An array of exit fiber lengths is calculated as shown in (13). Equation (14) results in the maximum exit fiber length. The array of exit fiber length error is the difference between the maximum exit fiber length and the array of exit fiber lengths, as shown in (15). Equation (16) results in the exit maximum fiber length error. The exit maximum fiber length error is multiplied by the integral gain and added to the previous entry flatness system proportional gain to calculate a new entry flatness system proportional gain as shown in (17). Adjusting the entry flatness system proportional gain will slowly adjust the leveler to achieve flat material. The integral gain would have to be very small to prevent the entry commanded offsets from changing rapidly.

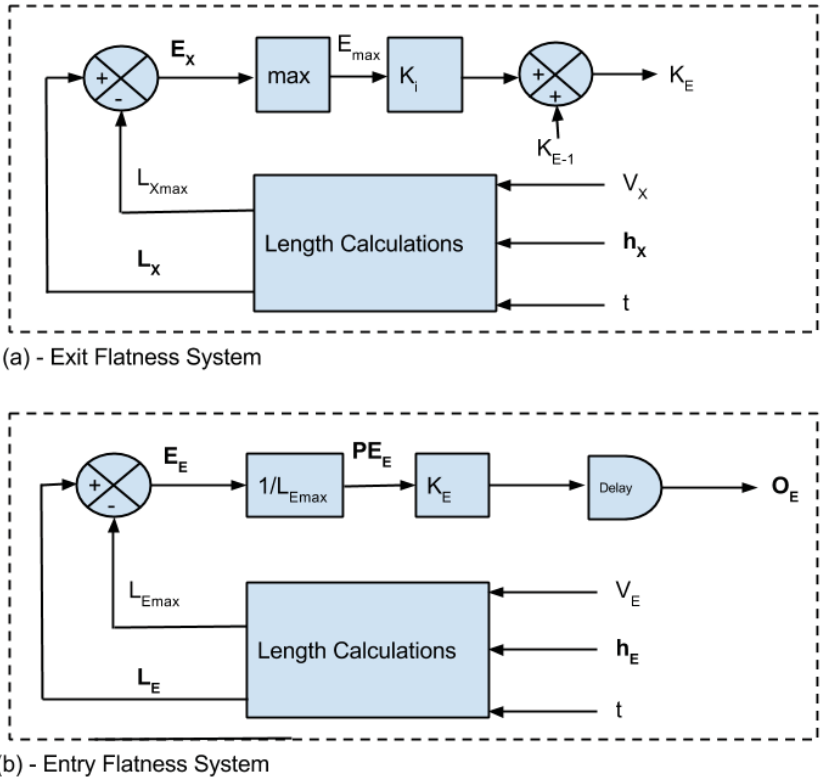

Figure 21: Control diagram for (a) exit flatness system as feedback for adaptation of proportional gain used in (b) entry flatness system.

$$\boldsymbol{L_X} = \begin{bmatrix} \sum_{j=1}^{m} \sqrt{\left(h_{X0,j} - h_{X0,j-1}\right)^2 + {v_{Xj}}^2 \cdot \left(t_j - t_{j-1}\right)^2} \\ \sum_{j=1}^{m} \sqrt{\left(h_{X1,j} - h_{X1,j-1}\right)^2 + {v_{Xj}}^2 \cdot \left(t_j - t_{j-1}\right)^2} \\ \sum_{j=1}^{m} \sqrt{\left(h_{X2,j} - h_{X2,j-1}\right)^2 + {v_{Xj}}^2 \cdot \left(t_j - t_{j-1}\right)^2} \\ \vdots \\ \sum_{j=1}^{m} \sqrt{\left(h_{Xn-1,j} - h_{Xn-1,j-1}\right)^2 + {v_{Xj}}^2 \cdot \left(t_j - t_{j-1}\right)^2} \end{bmatrix} \tag{13}$$

where

$\boldsymbol{L_X}$	exit fiber lengths of *n* backup flights (inches);
$h_{Xn,j}$	exit sensor height, flight number *n*, sample number *j* (inches);
v_{Xj}	exit strip speed, sample number *j* (inches per second);
t_j	time at sample *j* (seconds);
n	number of flights;
m	total number of samples;
j	current sample number.

$$L_{Xmax} = \max\left(L_{X0}, L_{X1}, L_{X2}, \ldots, L_{Xn-1}\right) \tag{14}$$

where

L_{Xmax}	exit maximum fiber length (inches);
L_{Xn}	exit fiber length of flight *n* (inches);
n	flight number.

$$\boldsymbol{E_X} = \begin{bmatrix} L_{X0} - L_{Xmax} \\ L_{X1} - L_{Xmax} \\ L_{X2} - L_{Xmax} \\ \vdots \\ L_{Xn-1} - L_{Xmax} \end{bmatrix} \tag{15}$$

where

$\boldsymbol{E_X}$	exit fiber length error (inches);
L_{Xn}	exit fiber length of flight *n* (inches);
L_{Xmax}	exit maximum fiber length (inches);
n	flight number.

$$E_{Max} = \max\left(E_{X0}, E_{X1}, E_{X2}, \ldots, E_{Xn-1}\right) \tag{16}$$

where

E_{Max} exit maximum fiber length error (inches);
E_{Xn} exit fiber length error of flight *n* (inches);
n flight number.

$$K_E = \left(E_{Max} \cdot K_i\right) + K_{E-1} \tag{17}$$

where

K_E entry flatness system proportional gain;
E_{Max} exit maximum fiber length error (inches);
K_i integral gain;
K_{E-1} previous entry flatness system proportional gain.

3.5 Adaptive control feedback from operator

Another method of feedback would be to capture the leveler offsets that the operator manually sets and compare these to the offsets that the entry flatness system calculates. This method assumes that the operator will not allow bad material to run. This is an excellent assumption as the cost of a coil of steel could be as much as $10,000. The manually adjusted offsets could be evaluated with the control system shown in figure 22. The difference between the entry flight calculated position offset array and the operator entered offset array yields the operator entered position offset error array as shown in (18). Equation (19) calculates the maximum operator entered position offset error. The maximum operator entered position offset error is multiplied by the integral gain and added to the previous entry flatness system proportional gain to calculate a new entry flatness system proportional gain as shown in (20). Adjusting the entry flatness system proportional gain will slowly adjust the leveler to achieve flat material. The integral gain, K_I, must be very small to slowly change

the proportional gain, K_E and prevent the entry commanded offsets from changing rapidly in the future.

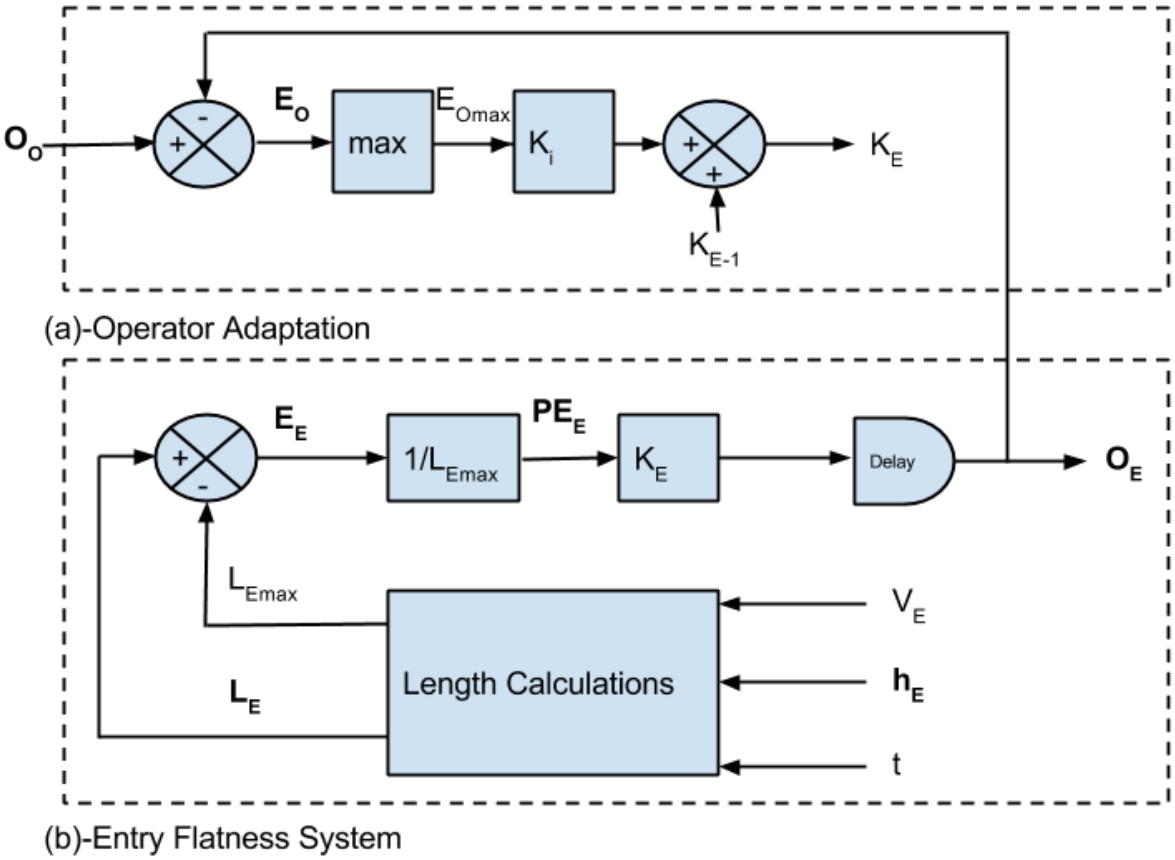

Figure 22: Control diagram for (a) operator entered offsets as feedback for adaptation of proportional gain used in (b) entry flatness system.

$$\boldsymbol{E_O = O_O - O_E} \tag{18}$$

where

$\boldsymbol{E_O}$	operator entered position offset error (inches);
$\boldsymbol{O_O}$	operator entered position offsets (inches);
$\boldsymbol{O_E}$	entry flight calculated position offset (in).

$$E_{Omax} = \max\left(E_{O0}, E_{O1}, E_{O2}, \ldots, E_{On-1}\right) \tag{19}$$

where

E_{Omax} maximum operator entered position offset error (inches);
E_{On} operator entered position offset error of flight *n* (inches);
n flight number.

$$K_E = \left(E_{Omax} \cdot K_i\right) + K_{E-1} \tag{20}$$

where

K_E entry flatness system proportional gain;
E_{Omax} maximum operator entered position offset error (inches);
K_i integral gain;
K_{E-1} previous entry flatness system proportional gain.

3.6 Proportional gain relationship versus material properties

In order for the adaptive control to work, the material properties would have to remain constant. The following are properties that can affect how much offset corrects a certain amount of elongation error.

1. Yield strength.
2. Modulus of Elasticity.
3. Material Thickness.

To calculate a vast range of entry flatness system proportional gains that would be needed for each combination of the above material properties would be time consuming and tricky. An alternative to this would be using operator's initial feedback as a method of selecting an entry flatness system proportional gain to start with as shown in the control system in figure 23.

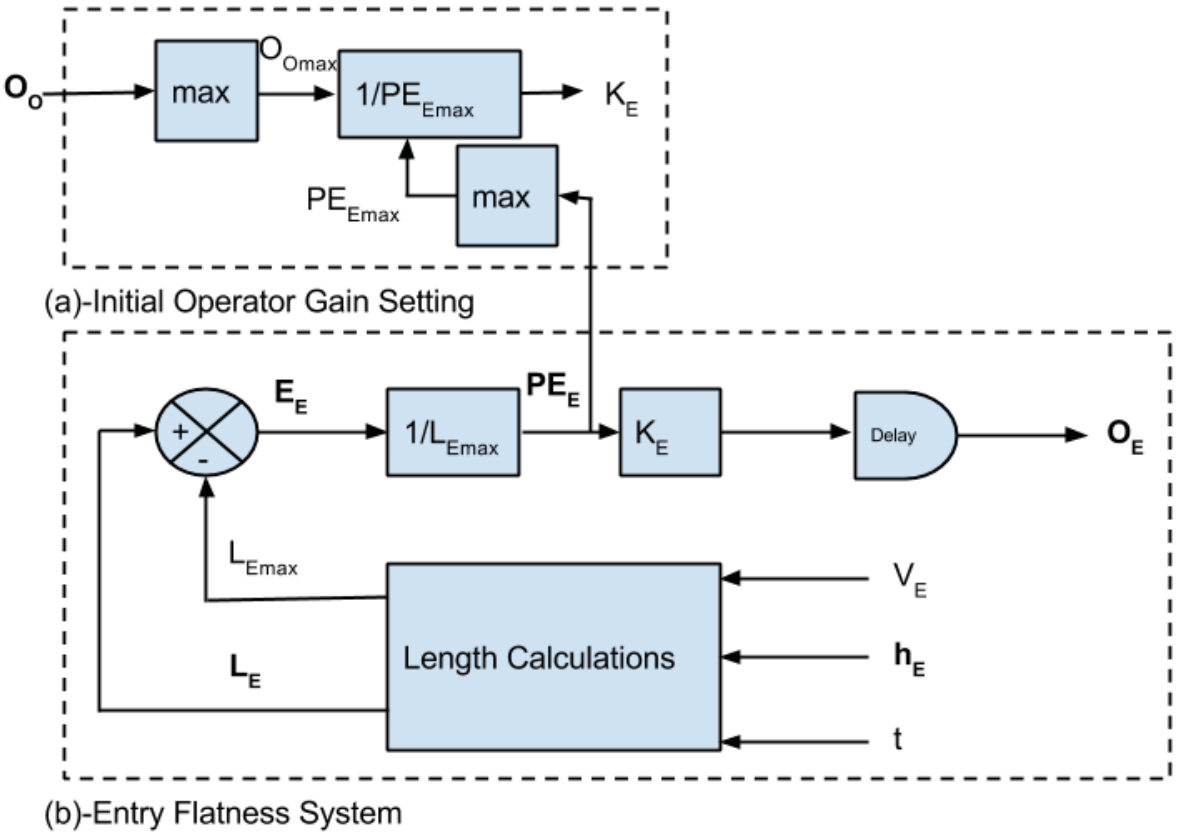

Figure 23: Control diagram of (a) operator setting the initial proportional gain to be used in (b) entry flatness system.

At the start of a coil, after the leveler is threaded, the operator will manually adjust the offsets. He will run the material back and forth in order to achieve acceptable shape coming out of the leveler. Once acceptable shape is obtained the operator will then start running the coil. The operator could initiate the control system shown in figure 23. The maximum operator entered position offset is calculated as shown in (21). Equation (22) yields the maximum entry fiber length percentage error. Dividing the two, as shown in (23), will result in the entry flatness system proportional gain.

$$O_{Omax} = \max\left(O_{O0}, O_{O1}, O_{O2}, \ldots, O_{On-1}\right) \tag{21}$$

where

O_{Omax} maximum operator entered position offset (inches);
O_{On} operator entered position offset of flight *n* (inches);
n flight number.

$$PE_{Emax} = \max\left(PE_{E0}, PE_{E1}, PE_{E2}, \ldots, PE_{En-1}\right) \tag{22}$$

where

PE_{Emax} maximum entry fiber length percentage error (%);
PE_{En} entry fiber length percentage error of flight *n* (%);
n flight number.

$$K_E = O_{Omax} \cdot \frac{1}{PE_{Emax}} \tag{23}$$

where

K_E entry flatness system proportional gain;
O_{Omax} maximum operator entered position offset (inches);
PE_{Emax} maximum entry fiber length percentage error (%).

3.7 Entry flatness system with adaptive control and operator initialization

The most complete control system would be one that combines the entry flatness system with adaptive control from the exit flatness system and operator initialization of the entry flatness system proportional gain as shown in figure 24. The operator can initialize the system to achieve acceptable shape, but then allow the exit flatness system to integrate the gain as shown in (24).

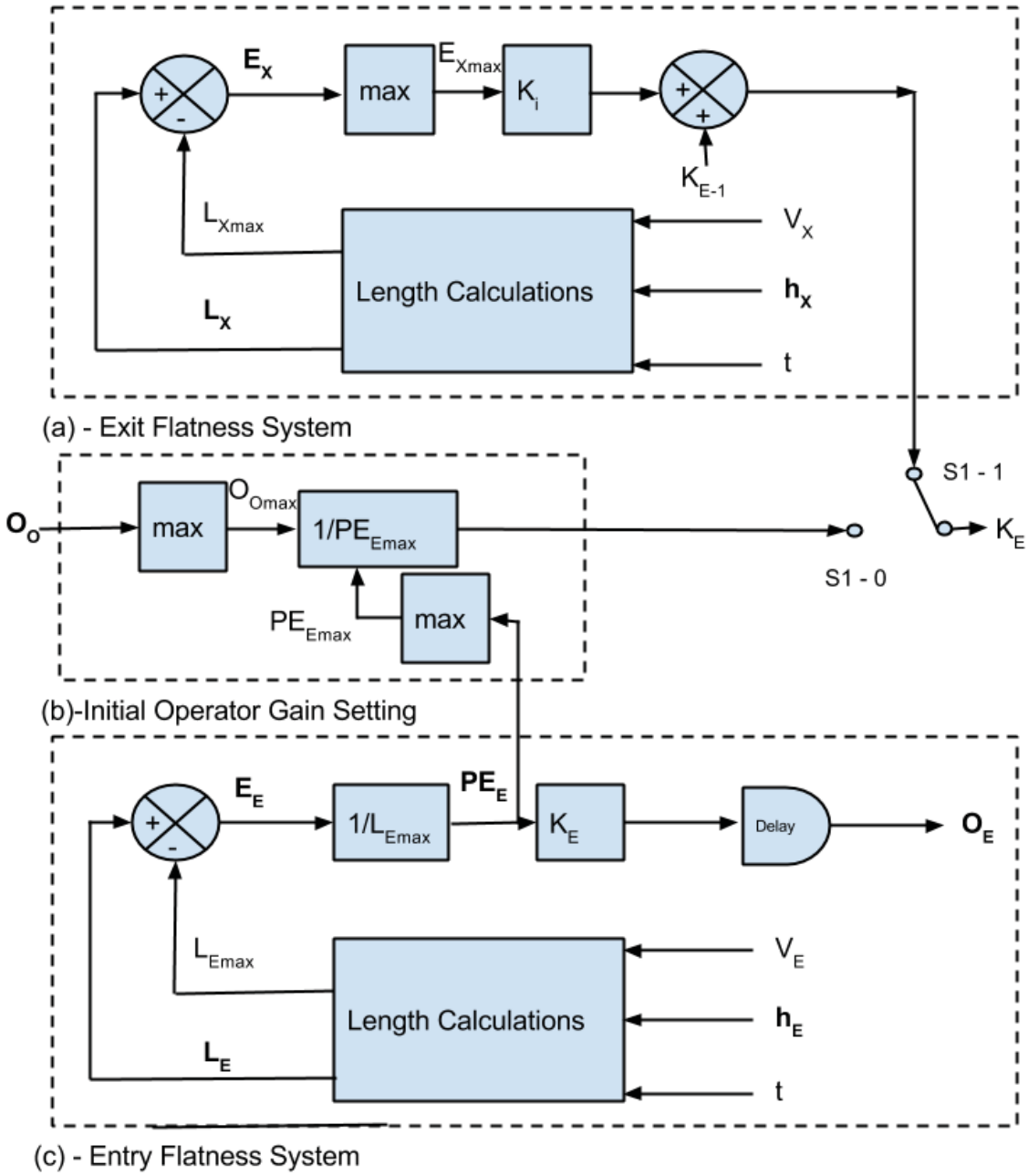

Figure 24: Control diagram of (a) exit flatness system as adaptive feedback with (b) operator setting the initial proportional gain to be used in (c) entry flatness system.

$$K_E = O_{Omax} \cdot \frac{1}{PE_{Emax}} \qquad S1 = 0$$
$$K_E = (E_{Xmax} \cdot K_i) + K_{E-1}, \qquad S1 = 1 \tag{24}$$

where

K_E	entry flatness system proportional gain;
O_{Omax}	maximum operator entered position offset (inches);
PE_{Emax}	maximum entry fiber length percentage error (%);
E_{Xmax}	maximum exit fiber length position error (inches);
K_i	integral gain;
K_{E-1}	previous entry flatness system proportional gain;
$S1$	operator initialization switch.

CHAPTER IV

IMPLEMENTATION OF BANK OF SENSORS

4.1 Overview

A bank of sensors was constructed and used for quality control in a manufacturing facility. This bank of sensors is similar to the bank of sensors that would be used for the purpose of this work with the exception that the bank of sensors installed is located after the leveler, not before.

4.2 Hardware used

The input of the non-contact sensor must occur at a high frequency due to the measurement technique of summing the distances to calculate the length of material feeding underneath a sensor. Most PLC's do not capture analog inputs at a rate that is adequate for this calculation. However, a dedicated digital acquisition device directly connected to a multi-core computer can capture data very quickly.

The device that was chosen for this analog input is the National Instruments X Series USB-6343 digital acquisition device. The product specification for this device can be found in Appendix A.1. This device can be controlled through the .NET programming

environment. This allows a custom .NET program to interface with it at very high speeds. An example of this acquisition code can be found in Appendix B.

The detection of depth of strip can be accomplished with either a laser or ultrasonic sensors. For this work, a Keyence IL-300 laser distance sensor was used. The product specification for this device can be found in Appendix A.2.

However, the laser is an expensive option. An ultrasonic sensor would be a more cost-effective option. For an ultrasonic test a Sick UM-18 sensor is used. Figure 25 shows a bank of ultrasonic sensors installed below the strip at a customer's site. At this site, the sensors were used to show an instantaneous graphical depiction of material profile. The product specification for this device can be found in Appendix A.3.

The leveler control is done with a standard programmable logic controller (PLC). The PLC used typically is an Allen-Bradley Controllogix PLC as shown in figure 26. The product specification for this device can be found in Appendix A.4.

Figure 25: Bank of ultrasonic sensors installed on site.

Figure 26: Allen-Bradley Controllogix PLC.

4.3 Testing

Two test units have been deployed to customer sites. These units are set to log data into files for later review and simulation. The information logged at time stamped intervals is given in table 4.

Table 4: List of data to be logged for simulation use.

Signal	**Units**	**Source**
Timestamp	Date (HH:MM:SS.MSMS)	NI Daq
Sensor Depth to Strip	Inches	NI Daq
Line speed	Inches per Second	Controllogix PLC
Material Width	Inches	Controllogix PLC
Material Thickness	Inches	Controllogix PLC
Material Modulus of Elasticity		Controllogix PLC
Material Yield Strength	PSI	Controllogix PLC
Leveler Entry Plunge	Inches	Controllogix PLC
Leveler Individual Flight Offsets	Inches	Controllogix PLC

The data given in table 4 has been logged into several files grouped by coil. This data was reviewed and deemed to be reasonable. However, due to the location of the sensor bank after the leveler, a simulation cannot be performed. The data that was collected coincides well with the material shape; however no quantitative analysis was possible due to the relatively flat nature of the material after being processed by the leveler. From the data logged and reviewed, it can however be asserted that the sensor bank is capable of measuring the shape of the material.

CHAPTER V

CONCLUSION

5.1 Accomplishments

The method of measuring the shape using the non-contact bank of sensors is an improvement compared to contact sensors. Non-contact sensors do not require tension to be applied to the strip in the measurement zone which can lead to measurement error. The non-contact sensors are not prone to vibration problems, which can also lead to measurement error. The adaptive control system, once developed further has the potential for improvement as well.

5.2 Improvements before true implementation

To truly call this a closed loop system, it should not rely solely on the operator to initially setup the leveler to achieve acceptable results. A method for capturing and modeling the effect of material properties on both the initial plunge of entry flights and individual flight offsets would need to be devised. Perhaps using the operator entered settings initially and logging the data would allow for a model to be calculated afterwards.

Also, this control scheme can neither detect nor correct for crossbow. No change in fiber length would be detected during crossbow. An additional method of detection would

have to be implemented, perhaps looking at the overall shape difference between sensors at snapshots.

Another problem is that we are assuming that the work rolls are bending to exactly the location of the flight. The movement of one flight affects the strip at the flights adjacent to it, and maybe the flights adjacent to those. A method of determining the effect that one flight has on the strip at the adjacent flights locations would have to be developed and implemented. Perhaps running some material with only one flight plunged deeper than the others and capturing the results on the exit flatness system would suffice.

5.3 Summary

The bank of sensors designed here, along with the shape detection algorithms conceived should provide a good starting point for an automatic shape control system for a roller leveler. The actual closed loop portion would require some more work as detailed above. If the above improvements are made, then perhaps the years of training and experience necessary for an operator to become skilled could be reduced dramatically. This reduction in skill required to achieve acceptable material flatness, would be a very important development in leveling.

APPENDIX A

Hardware Cut Sheets

This appendix includes the cut sheets for the National Instruments data acquisition unit, the Keyence distance laser, the Sick ultrasonic sensor, and the Allen-Bradley Controllogix PLC.

A.1 NI USB-6343 X Series Data Acquisition Cut Sheet

- BNC connectivity now available!
- 32 analog inputs, 500 kS/s, 16-bit resolution, ±10 V
- Four analog outputs, 900 kS/s, 16-bit resolution, ±10 V
- 48 digital I/O lines (32 hardware-timed up to 1 MHz)
- Four 32-bit counter/timers for PWM, encoder, frequency, event counting, and more
- Advanced timing and triggering with NI-STC3 timing and synchronization technology
- Support for Windows 7/Vista/XP

Overview

NI X Series multifunction data acquisition (DAQ) devices for USB provide a new level of performance with NI-STC3 timing and synchronization technology, NI Signal Streaming for high performance over USB, a completely redesigned mechanical enclosure, and multicore-optimized driver and application software.

NI-STC3 Technology

NI-STC3 timing and synchronization technology delivers advanced timing features, including independent analog and digital timing engines, retriggerable measurement tasks, and four counter/timers with more functionality than ever before.

NI Signal Streaming

USB X Series devices include patented NI Signal Streaming, a technology that uses message-based instructions and device-side intelligence to ensure high-speed, bidirectional data transfer over USB. With USB X Series, you can concurrently transfer analog, digital, and counter data in both directions.

Data Acquisition Software

X Series devices include multithreaded NI-DAQmx driver software, which is compatible with the following versions (or later) of NI application software - LabVIEW 8.5, LabWindows™/CVI 8.1, or Measurement Studio 8.0.1; or LabVIEW SignalExpress 2.x. X Series devices are also compatible with ANSI C/C++ and Microsoft Visual Studio .NET. NI-DAQmx includes free LabVIEW SignalExpress LE data-logging software and hundreds of shipping examples to help you get started quickly with your application.

Specifications

Specifications Documents

- Specifications
- Data Sheet

Specifications Summary

General	
Product Name	USB-6343
Product Family	Multifunction Data Acquisition
Form Factor	USB
Part Number	781439-01
Operating System/Target	Windows
LabVIEW RT Support	No
DAQ Product Family	X Series
Measurement Type	Digital , Voltage , Frequency , Quadrature encoder
Isolation Type	None
RoHS Compliant	Yes
USB Power	External-Powered
Termination Type	Screw-Termination
Power Supply	Yes
Enclosure Type	Metal
Analog Input	
Channels	32 , 16
Single-Ended Channels	32
Differential Channels	16
Resolution	16 bits
Sample Rate	500 kS/s
Throughput (All Channels)	500 kS/s
Number of Ranges	4

Simultaneous Sampling	No
Analog Output	
Channels	4
Resolution	16 bits
Update Rate	900 kS/s
Current Drive Single	5 mA
Digital I/O	
Bidirectional Channels	48
Input-Only Channels	0
Output-Only Channels	0
Timing	Software , Hardware
Clocked Lines	32
Maximum Clock Rate	1 MHz
Logic Levels	TTL
Input Current Flow	Sinking , Sourcing
Output Current Flow	Sinking , Sourcing
Programmable Input Filters	Yes
Supports Programmable Power-Up States?	Yes
Current Drive Single	24 mA
Current Drive All	1 A
Watchdog Timer	Yes
Supports Handshaking I/O?	No
Supports Pattern I/O?	Yes
Maximum Input Range	0 V , 5 V
Maximum Output Range	0 V , 5 V
Counter/Timers	
Counters	4
Buffered Operations	Yes
Debouncing/Glitch Removal	Yes

GPS Synchronization	No
Maximum Range	0 V , 5 V
Max Source Frequency	100 MHz
Pulse Generation	Yes
Resolution	32 bits
Timebase Stability	50 ppm
Logic Levels	TTL
Physical Specifications	
Length	26.4 cm
Width	17.3 cm
Height	3.6 cm
I/O Connector	Screw terminals
Timing/Triggering/Synchronization	
Triggering	Digital
Synchronization Bus (RTSI)	No

A.2 Keyence IL-300 Analog Displacement Laser Cut Sheet

Model		IL-300
Reference distance		300 mm 11.81”
Measurement range		160 to 450 mm 6.30” to 17.72”
Light source	Type	Red semiconductor laser, wavelength: 655 nm (visible light)
	Laser class	Class 2 (FDA (CDRH) Part1040.10)*6 Class 2 (IEC 60825-1)
	Output	560 µW
Spot diameter (at standard distance)		Approx. ø0.5 mm ø19.7 Mil
Linearity*1*2		±0.25% of F.S.
Repeatability*3		30µm1.18 Mil
Sampling rate		0.33/1/2/5 ms (4 levels available)
Operation status indicators		Laser emission warning indicator: Green LED, Analog range indicator: Orange LED, Reference distance indicator: Red/Green LED
Temperature characteristics*4		0.08% of F.S./°C
Environmental resistance	Enclosure rating	IP67
	Ambient light*5	Incandescent lamp: 5000 lux
	Ambient temperature	-10 to +50°C (14 to 122°F) (No condensation or freezing)
	Relative humidity	35 to 85% RH (No condensation)
	Vibration	10 to 55 Hz 1.5 mm 0.06" double amplitude in the X, Y and Z directions, 2 hours respectively
Material		Housing material: PBT Metal parts: SUS304 Packing: NBR Lens cover: Glass Cable: PVC
Weight		Approx. 135 g

*1 Value when measuring the KEYENCE standard target (white diffuse object).

*2 The F.S. of each model is as shown to the right. IL-S025/IL-030: ±5 mm, IL-S065/IL-065: ±10 mm, IL-100: ±20 mm, IL-S100: ±30 mm, IL-300: ±140 mm, IL-600: ±400 mm,

IL-2000: +1000 to -1500 mm

*3 Is the value for when our standard object (white diffuse object) is measured at an average of 128 times and with a sampling rate of 1 ms from a standard distance. (IL-300/

IL-600 is 2 ms and IL-2000 is 5 ms).

*4 F.S. for each model is as follows: IL-030: ±5 mm 0.20" IL-065: ±10 mm 0.39" IL-100: ±20 mm 0.79" IL-300: ±140 mm 5.51" IL-600: ±400 mm 15.75"

*5 Value when the sampling rate is set to 2 ms or 5 ms.

*6 The laser classification for FDA (CDRH) is implemented based on IEC 60825-1 in accordance with the requirements of Laser Notice No.50.

[*7] Amplifiers purchased before August 8th, 2012 cannot be used.

A.3 Sick UM18 Ultrasonic Sensor Cut Sheet

SICK
Sensor Intelligence.

Ultrasonic sensors
UM18, UM18-2 Pro, IO-Link

Model Name > UM18-212126111
Part No. > 6048398

At a glance

- Reliable measurement independent of material color, transparency, gloss and ambient light
- Four ranges up to 1,300 mm
- Short M18 metal housing with a length of 41 mm
- Straight or right-angle versions
- Analog voltage, analog current or push-pull (PNP/NPN in one) switching output with IO-Link available
- Set-up via IO-Link and/or teach-in via multifunction input
- High immunity to dirt, dust, humidity and fog

Your benefits

- Ranges up to 1,300 mm offer plenty of options for flexible use
- Easy machine integration due to short M18 housing available in straight or right-angle versions
- Intelligent measurement filters ensure reliable measurement results for highest process stability
- Integrated temperature compensation ensures high measurement accuracy at any time for best process quality
- Solid, one-piece metal housing secures highest machine availability
- Synchronization or multiplexing allow simultaneous use of up to 10 sensors, which improves application flexibility and process stability
- Unintentional adjustments to sensor settings are eliminated since teach-in process is done with an external wire
- Devices with switching output and IO-Link allow highest machine flexibility while offering easy machine operation

Performance

Resolution:	≥ 0.069 mm
Working range, limiting range:	65 mm ... 350 mm, 600 mm
Repeatability [1]:	± 0.15 %
Accuracy [2]: [3]:	± 1 %
Response time:	64 ms
Output rate:	16 ms
Ultrasonic frequency (typical):	400 kHz
Detection area (typical):	See diagrams
Temperature compensation:	✓

Additional function:	Teach-in of analog output Temperature compensation Synchronization of up to 10 sensors Multiplexing: no cross talk of up to 10 sensors Reset to factory default Multifunctional input: external teach/synchronization/multiplexing Invertible analog output

[1] [2] Referring to current measurement value [3] Temperature compensation can be switched off, without temperature compensation: 0.17 %/K

Interfaces

Analog output [1]; [2]:	1 x 4 mA ... 20 mA (≤ 500 Ω)
Resolution analog output:	12 bit
Hysteresis:	5 mm
Multifunctional input (MF):	1 x MF
Data interface:	IO-Link
BETRIEBSREICHWEITE-GR.COLL:	65 mm 350 mm 600 mm

[1] For 4 mA ... 20 mA and V_S ≤ 20 V max. load ≤ 100 Ω [2] Subsequent smoothing of the analog output, depending on the application, may increase the response time by up to 200 %

Mechanics/electronics

Sending axis:	Straight
Supply voltage Vs [1]; [2]:	DC 10 V ... 30 V
Power consumption [3]:	≤ 1.2 W
Initialization time:	< 300 ms
Housing material:	Nickel-plated brass ultrasonic transducer: polyurethane foam, glass epoxy resin
Connection type:	Male connector, M12, 5-pin
Indication:	2 x LED
Weight:	25 g

[1] Limit values, reverse-polarity protected, operation in short-circuit protected network: max. 8 A [2] 15 V ... 30 V when using analog voltage output [3] Without load

Ambient data

Enclosure rating:	IP 67
Protection class:	III
Ambient temperature:	Operation: -25 ... 70 °C Storage: -40 ... 85 °C

A.4 Allen-Bradley Controllogix Cut Sheet

ControlLogix Standard Controllers

Bulletin 1756 ControlLogix® Standard Controllers are suitable for process, motion, discrete, and high-availability applications. As part of the Rockwell Automation® Integrated Architecture™ system, the L6x and L7x models use RSLogix™ 5000 programming software and common network protocols, and they offer common information capabilities. These high-performance controllers provide a common control engine with a common development environment for all control disciplines. Consider these controllers for more sophisticated machines and for connectivity to business systems.

Overview Software Documentation Resources Accessories Applications

Features

- Provide twice the processing speed in the L7x models when compared to the L6x models
- Support Integrated Motion on EtherNet/IP™, integrated Sercos™ motion, and analog motion
- Support full controller redundancy
- Support removal and insertion under power (RIUP)
- Communicate via EtherNet/IP, ControlNet™, DeviceNet™, Data Highway Plus™, Remote I/O, SynchLink, and third-party process and device networks
- Let you program using relay ladder logic, structured text, function block, and SFC languages
- Offer flexible user memory options

Products

- 1756 ControlLogix® Standard Controllers, L7x and L6x models

ControlLogix Standard Controller Comparison

Feature	L7x Models	L6x Models
Performance Capability	Twice the performance of L6x models	High
Max. Controller Connections	500	250
Built-in Port	USB	Serial
Energy Storage Module (ESM) Included	Yes	No
Battery Required	No	Yes
On-board Display Included	Yes	No
Non-volatile Memory	Secure Digital card	CompactFlash card
Max. User Memory	32 MB	32 MB
Max. I/O Points	128,000 digital; 4,000 analog	128,000 digital; 4,000 analog
I/O Module Integration	1756 ControlLogix I/O	1756 ControlLogix I/O

Certifications

- ControlLogix Standard Controllers, L7x models: c-UL-us, CE, C-Tick, ATEX, KC, FM
- ControlLogix Standard Controllers, L6x models: c-UL-us, CSA,CE, C-Tick, ATEX, KC

APPENDIX B

Example of .NET code for NI-DAQ USB-6343

Example code is given in the VB.NET programming language. The code snippets are for creating an analog input task using the National Instruments digital acquisition library, capturing the analog input data, and closing and disposing of the analog input task.

B.1 Creating an analog input task

```
   Public Sub ai_init()

        'create a new custom scale for the sensors
        Dim AIscale As Scale = New RangeMapScale("ai_scale", min_voltage, max_voltage,
min_distance_inches, max_distance_inches)

        AIscale.PreScaledUnits = ScalePreScaledUnits.Volts

        AIscale.ScaledUnits = "inches"


           'Create analog Input task
           ai_Task = New Task()

           ai_Task.AIChannels.CreateVoltageChannel(daq_path & "ai0", "Sensor 1",
term_config, min_distance_inches,  max_distance_inches,
AIVoltageUnits.FromCustomScale)

           'set scale to inches
           ai_Task.AIChannels(0).CustomScaleName = "ai_scale"

           'Verify the Task
           ai_Task.Control(TaskAction.Verify)

           'set up the analog input reader
           ai_reader = New AnalogMultiChannelReader(ai_Task.Stream)

           'setup callback function evertime a new sample occurs
           ai_Callback = New AsyncCallback(AddressOf ai_Callback_Fnc)


           ai_reader.SynchronizeCallbacks = True

           ai_reader.BeginReadSingleSample(ai_Callback, vbNull)

           'start the task
           ai_Task.Start()

      End Function
```

B.2 Capturing Data from an Analog Input Task

```
    Private Function ai_Callback_Fnc(ByVal ar As IAsyncResult) As Integer

        Try
            Dim ai_Data As Double()
            If (Not (ai_Task Is Nothing)) Then
                'get data from last sample
                ai_Data = ai_reader.EndReadSingleSample(ar) ‘This would be an array of
sensor data in inches

                'set the async callback for the next sample
                ai_reader.BeginReadSingleSample(ai_Callback, vbNull)

            End If
        Catch ex As Exception
            Return LOG_FAILED_TO_CAPTURE_AI 'Create Failed
            Exit Function
        End Try

        Return RETURN_OK

    End Function
```

B.3 Closing and disposing of analog input task

```
    Public Function cleanup() As Integer


        'Cleanup Analog Inputs (Lasers)
        Try
            If (Not (ai_Task Is Nothing)) Then

                ai_Task.Stop()
                ai_Task.Dispose()
                ai_Task = Nothing

            End If
        Catch ex As Exception
          Return LOG_FAILED_TO_DISPOSE_AI 'Create Failed
        End Try

        Return RETURN_OK

    End Function
```

REFERENCES

[1] J. R. Buta, "Roller Leveler and Method of Operating Same". United States of America Patent 4454738, 19 June 1984.

[2] F. K. Maussnest, "Method and Appartus for Straightening Sheet Material". United States of America Patent 2009508, 30 July 1935.

[3] G. C. Bergman and A. D. Enneking, "Displacement-type shape sensor for multi-roll leveler". United States of America Patent 6857301, 22 February 2005.

[4] J. W. Reesor, "Automatic control and indicating systems for roller levelers". United States of America Patent 3416340, 17 December 1968.

[5] E. Theis, "Everything you need to know about flatteners and levelers for coil processing—Part 1," Fabricator, 12 October 2002. [Online]. Available: http://www.thefabricator.com/article/coilprocessing/everything-you-need-to-know-about-flatteners-and-levelers-for-coil-processing-part-1. [Accessed 5 November 2013].

[6] T. R. Lloyd, "Roller leveler machine". United States of America Patent 2429142, 14 October 1947.

[7] E. Theis, "Everything you need to know about flatteners and levelers for coil processing—Part 3," Fabricator, 16 January 2003. [Online]. Available: http://www.thefabricator.com/article/coilprocessing/everything-you-need-to-know-about-flatteners-and-levelers-for-coil-processing-part-3. [Accessed 5 November 2013].

[8] E. Theis, "Everything you need to know about flatteners and levelers for coil processing—Part 2," Fabricator, 7 November 2002. [Online]. Available: http://www.thefabricator.com/article/coilprocessing/everything-you-need-to-know-about-flatteners-and-levelers-for-coil-processing-part-2. [Accessed 5 November 2013].

[9] B. Cox, "Roller Leveling 101," Stamping Journal, 13 March 2007. [Online]. Available: http://www.thefabricator.com/article/stamping/roller-leveling-101. [Accessed 13 August 2014].